The β-factor: Measuring Wireless Link Burstiness

Kannan Srinivasan, Maria A. Kazandjieva, Saatvik Agarwal, Philip Levis
Computer Systems Lab
Stanford University
Stanford, CA 94131
{srikank,mariakaz,legolas}@stanford.edu, pal@cs.stanford.edu.

Abstract

Measuring 802.15.4 reception in three testbeds, we find that most intermediate links are bursty: they shift between poor and good delivery. We present a metric to measure this link burstiness and name it β. We find that link burstiness affects protocol performance and that β can predict the effects. We show that measuring β allows us to reason about how long a protocol should pause after encountering a packet failure to reduce its transmission cost. We find that using β as a guide to setting a single constant in a standard sensor network data collection protocol reduces its average transmission cost by 15%. In addition to data from 802.15.4 testbeds, we examine traces from 802.11b networks and find β has a broader relevance in the wireless domain.

1 Introduction

Link burstiness can greatly affect protocol performance. For example, MAC-layer immediate retransmissions are much less effective on links with bursts of losses than on links with independent losses. This means that two networks can have identical connectivity and packet reception ratio, yet exhibit completely different performance. Despite the fact that many protocol studies have shown wireless links to be bursty [2, 5, 17, 19, 26] and that this burstiness affects experimental results, there is no well-established burstiness metric. Such a metric will help understand why some protocols behave differently on similar networks and will provide insights into tuning protocol parameters to improve performance.

There is a long history of quantifying burstiness at lower layers of the protocol stack. At the physical layer, coherence time [12] describes the interval over which a signal is correlated. The Gilbert-Elliott model, a two-state Markov chain, presents burstiness in terms of μ, effectively describing how bit errors are correlated [22]. We defer a more detailed discussion of existing approaches to Section 8.

The major departure this paper takes from prior work is that it is experimental rather than analytic: it seeks to define a *metric* rather than a *parameter*. Coherence time and μ, for example, are parameters to analytical equations that model protocol performance. In practice, protocol designers know that the real world is much more complex [17, 19]. Therefore, this paper examines how we can derive new metrics from measurements of a real network, measurements which exhibit all the complexities that analytical models are forced to avoid for tractability.

This paper has three research contributions. First, it describes an algorithm to measure link burstiness, β, and shows that β can predict protocol performance. Second, it shows how to use β to improve efficiency in bursty networks by tuning protocol parameters. We find that changing a single constant in TinyOS 2.0's standard collection protocol (CTP) can improve its transmission efficiency by 15%. Finally, it investigates the underlying causes of link burstiness and shows that variation in the signal to noise ratio is a possible cause.

We calculate β using conditional probability delivery functions (CPDFs) derived from packet delivery traces [20]. CPDFs give the probability a packet will be received successfully after n consecutive successes or failures. CPDFs can describe ideal bursty links, which have one long burst of either successes or failures, as well as independent links, in which there is no correlation between packet delivery events. β measures whether a link is closer to the independent or ideal bursty link: a high β means a link is very bursty, while a β close to zero means the link is independent. We defer a detailed description of how to calculate β to Section 3.

We explore how well β can predict protocol performance using a simple algorithm called *opportune transmissions*. Opportune transmissions increase the observed reception ratio of bursty links by sending packets back-to-back until a failure and by pausing after the failure. This approach trades off throughput and latency for reduced transmission cost. In a network with many high-β links, 25% of the links see reception ratio improvement of over 100%. However, in a network with fewer than 5% of the links with a β greater than 0.9, no links see improvement of 100% or more. As opportune transmissions are meant for bursty links, they work well in networks with many such links. This shows that β is capturing burstiness and it allows us to reason why protocols similar to opportune transmisisons would perform differently on different networks.

The timescale over which we observe links affects β; increasing the inter-packet interval in the data traces

decreases β – packet events become less correlated as the interval between the events increases. This suggests that looking at the decay of β can show when a link can resume transmissions upon a packet failure.

The path and link cost results come from the traces with which we calculated β. This raises the question of whether the same information from β can predict the performance of a protocol that runs after the network has been measured. Changing the pause interval of a standard sensornet collection protocol and running it in real-time on a testbed decreases the overall network delivery cost by 15%. This shows that β gives further insight into a network's characteristics and into how protocol designers can tune their protocols according to the network to improve performance.

Exploring the possible causes of burstiness in 802.15.4 reveals that it is due to channel variations, in the form of changes in received signal strength. As channel variations are common in wireless networks, β may be more broadly applicable than just 802.15.4. Examining data from 802.11b studies [7, 23], we find that 802.11b in both indoor and outdoor environments exhibits burstiness and that β can predict protocol performance in 802.11b networks.

Measuring burstiness and its effect on network performance suggest we need to rethink current approaches to wireless protocol design and analysis: reasoning about how protocols perform requires an understanding of fine-grained temporal properties.

The rest of this paper is structured as follows. Section 2 looks at reception ratios of wireless links. Then Section 3 quantifies link burstiness and introduces β. Section 4 presents a simple algorithm that can benefit from a knowledge of β. Section 5 investigates the causes of burstiness and Section 6 shows that this burstiness is relevant to different link layers. Section 7 further evaluates β's effect on protocols. Finally, Section 8 discusses related work and concludes.

2 802.15.4 Packet Delivery

This section introduces 802.15.4, its packet delivery behavior, and the testbeds we use. It also defines the terminology to describe links with different receptions and observes that the timescale of measurements affects testbed reception results.

2.1 802.15.4 and Testbeds

802.15.4 is an IEEE PHY-MAC standard for low power, low datarate networks. It has a datarate of 250kbps and a range of approximately one hundred meters. It provides 16 channels, numbered 11-26 in the 2.4 GHz band (2405 MHz - 2480 MHz). The channels are 5 MHz apart, overlapping with 802.11b and 802.15.1 (Bluetooth).

We measured 802.15.4 using three wireless sensornet testbeds. Most experiments use the 100 node Intel Mirage testbed [14]. We also present results from a 30 node university testbed; the Mirage and university nodes are on the ceiling. Finally, we examine an outdoor 20 node dry lake testbed in which nodes were arranged in a line, spaced 4 feet apart and all had clear line of sight. All nodes in these experiments ran TinyOS [13] and used the CC2420 802.15.4 chip [6], which provides variable transmit power control from 0dBm to -20dBm.

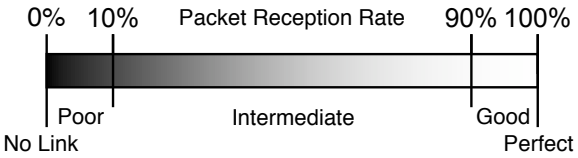

Figure 1. Terminology used to describe links based on PRR. Poor links have a PRR $< 10\%$, intermediate links are between 10% and 90%, and good links are $> 90\%$. A PRR of 100% is a perfect link. A link that receives one or more packets is a communicating link.

2.2 Packet Delivery

Prior studies of wireless networks have observed that links have a wide range of packet reception ratios (PRR) which can vary significantly over time [2, 4, 23, 21]. To determine whether 802.15.4 behaves similarly, we measured reception ratios in the university, Mirage and lake testbeds. In the rest of this paper, we describe links as poor, intermediate, good, or perfect in terms of PRR, using the definitions shown in Figure 1; we use the terms link quality and packet reception ratio interchangeably. Since prior studies have shown that 802.15.4 links can vary significantly over time [21], we measured reception ratios over different time scales by sending 200 broadcasts with varying inter-packet intervals (IPI, the time between packet transmissions). We used inter-packet intervals ranging from 10ms up to 15 seconds. All packets used the standard TinyOS CSMA layer and we controlled transmission timing so there would be no collisions. The lack of a wired backchannel prevented lake nodes from having an IPI below 50ms.

Figure 2(a) shows the reception ratio distribution in the three testbeds on channel 26 with small inter-packet intervals. About 55% of all node pairs in the Mirage and university testbeds can communicate, while 90% of the pairs in the lake testbed can communicate. Of these communicating links, 19% in Mirage, 14% in the lake, and 5% in the University are intermediate. These numbers are lower than what has been observed in other networks. Even the 19% in Mirage is much less than the 50% reported for earlier sensor platforms and the 58% reported for Roofnet [2]. Compared to these other networks, 802.15.4 has a much sharper reception distribution. While intermediate links do not dominate the network, wireless protocols cannot simply ignore them.

2.3 Time and Frequency Effects

Figures 2(b) and 2(c) show how the time interval between packets affects the reception ratio distribution. In-

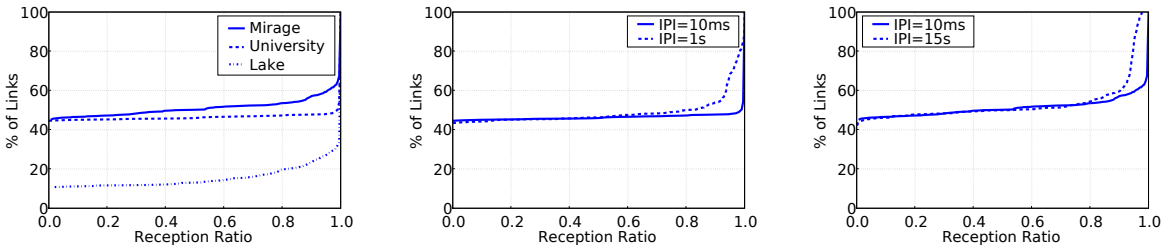

(a) University and Mirage IPI=10ms, Lake IPI=50ms (b) University (c) Mirage

Figure 2. Reception ratio and the CDF of proportion of links in the three testbeds for channel 26. The percentage of intermediate links is small compared to good and bad links, and it increases as the inter-packet interval increases.

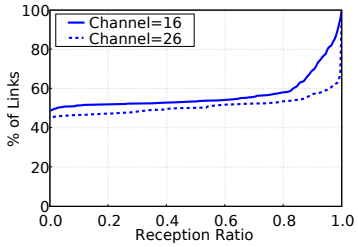

Figure 3. CDFs of link qualities in Mirage on Channels 16 and 26. The proportion of perfect links is more in channel 26 than in channel 16: 60% in 26 and 12% in 16 of all the communicating links.

creasing the IPI from 10ms to 1 second increases the percentage of intermediate links from 5% to 19% in the university testbed. Mirage increases from 19% to 23% as IPI increases from 10ms to 15 seconds. As the reception ratio is calculated over 200 packets, the packet interval determines the total measurement time: an experiment with IPI of 10ms takes 2 seconds while one with an IPI of 15 seconds takes 50 minutes.

Timing is not the only factor that affects link distributions. Figure 3 shows how channel selection changes the PRR distribution in Mirage. Channel 16 has far fewer perfect links than channel 26: 60% in channel 26 and only 12% in channel 16. Correspondingly, 35% of the communicating channel 16 links are intermediate, compared to 17% of channel 26 links.

These results lead to two major observations. First, frequency affects link distributions. While this is not surprising, learning *why* is an important step to better understand wireless behavior. We defer this question to Section 5.

Second, the percentage of intermediate links depends on the timescale over which a protocol measures them. Over shorter periods, links have a higher chance of being perfect or non-existent. Over longer periods, the chance of being intermediate increases. In Section 5, we examine this behavior more closely, finding it is due to links on the edge of reception sensitivity, moving between poor and good states. As the measurement period increases, so does the chance of observing a transition. While this is a simple observation, it has deep implications for wireless protocol design: the data plane may observe different link qualities than the control plane which sends link measurement packets.

3 Measuring Burstiness

This section defines β, a metric to measure links' bursty behavior. We show how to compute β and observe that many Mirage links on channel 26 have high β values.

3.1 Conditional Delivery

First, we need a way to concisely describe link behavior observed in packet traces. Conditional packet delivery functions (CPDFs) provide a succinct way to describe the durations of packet delivery correlations [20]. The conditional packet delivery function $C(n)$ is the probability the next packet will succeed given n consecutive packet successes (for $n > 0$) or failures (for $n < 0$). For example, $C(5) = 83\%$ means that the probability a packet will arrive after five successful deliveries is 83%, while $C(-7) = 18\%$ means that the probability after seven consecutive losses is 18%.

Figure 4 shows four sample CPDFs. A link with independent losses will have a flat CPDF: the probability of reception is independent of any history. In contrast, Figure 4(a) shows the CPDF of the ideal bursty link; successes and failures happen in bursts. There is an inherent timescale assumption in this description: the burst length must be longer than the CPDF x-axis range. Burst lengths that are small enough to occur within the CPDF range make a link look more independent.

We program nodes on the Mirage testbed to broadcast 100,000 packets with an inter-packet interval of 10ms, one node at a time, and use the packet traces to calculate link CPDFs. We use 100,000 packets to provide reasonable confidence intervals to the CPDF values. In addition, each element in a CPDF has a minimum of 100 data points.[1] Figures 4(b)-4(d) show the

[1] 100 data points gives a worst case 95% confidence interval of [p-0.1,p+0.1], where p is the empirical conditional probability.

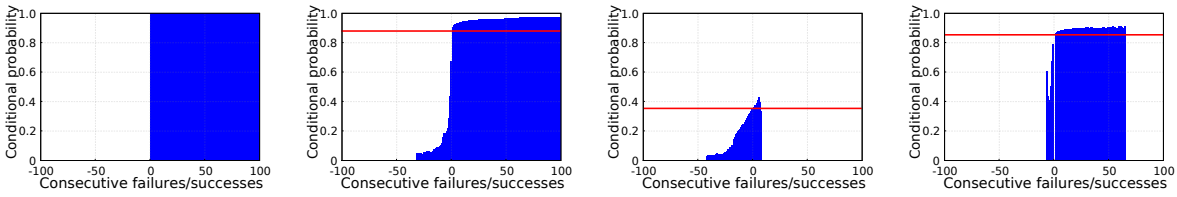

(a) KW= $0, \beta = 1$. (b) KW= $0.06, \beta = 0.8$. (c) KW= $0.20, \beta = 0.5$. (d) KW= $0.14, \beta = 0.3$.

Figure 4. CPDFs with their corresponding KW-distances and β value. The ideal bursty link is shown in (a), while (b)-(d) are links observed in the Mirage testbed. The red horizontal line shows the overall reception ratio of the link. Positive X-axis values are consecutive successes while negative X-axis values are consecutive failures.

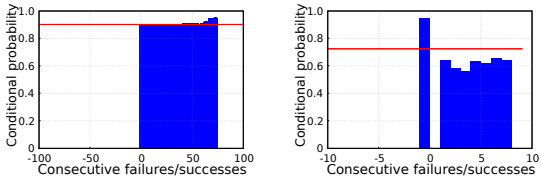

(a) KW=0.1, $\beta = 0$ (b) KW=0.45, $\beta = -0.36$ (note smaller x range)

Figure 5. Two link edge cases. Independent links with high or low reception ratios have a low distance but a β close to 0. Links with negative correlation have a $\beta < 0$.

CPDFs of three sample links. We do not assume any values for the CPDF elements that have fewer than 100 datapoints and do not consider them in our analysis. For example, the CPDF shown in Figure 4(c) does not have any values above 7 and below -42. We defer the discussion of CPDF's relationship with other statistical quantities to Section 8.

3.2 Kantorovich-Wasserstein

CPDFs distill a long vector of packet delivery successes and failures into a concise representation of burstiness. While CPDFs can give a good visual intuition of link behavior, we want to present burstiness as a single scalar value. To do so, we borrow an approach from [20] and use the Kantorovich-Wasserstein (KW) distance [24] to measure how close a CPDF is to that of the ideal bursty link (Figure 4(a)). In other words, the KW distance between two vectors is the average of the absolute differences of the corresponding elements of the two vectors. In the rest of this paper, when we refer to the distance of a link, we mean the KW distance from the ideal bursty link.

The captions in Figure 4 include the distances of the three example Mirage links. A CPDF that is further from the ideal bursty link has a larger distance. For example, Figure 4(d) has a larger distance than Figure 4(b) because the small number of data points with negative n values have reasonably high conditional probabilities.

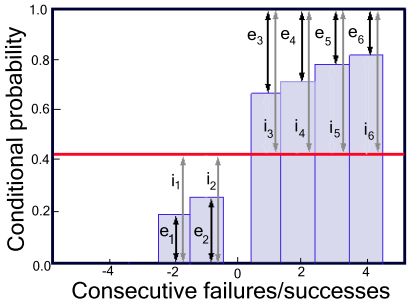

Figure 6. β calculation of an example link. The distances e_1 – e_6 are the distances between the CPDF elements of the example link and the CPDF elements of the ideal bursty link. The distances i_1 – i_6 are the distances between the CPDF elements of the corresponding independent link and the CPDF elements of the ideal bursty link. $\beta = \frac{mean(i_1,..,i_6) - mean(e_1,..,e_6)}{mean(i_1,..,i_6)}$.

3.3 β: The Burstiness Metric

While distance is informative, it is not sufficient to measure burstiness because CPDFs often do not have the same number of elements with positive and negative n values. For example, consider a link with a reception ratio of 90% whose packet deliveries are independent. Figure 5(a) shows the CPDF of such a link (synthetically generated with a random process), where the conditional probability is for the most part constant for all n. This hypothetical link, however, has a low distance of 0.1 from the ideal bursty link. There are many values for $n > 0$ that are close to the bursty link's 100%, while only a few values for $n < 0$, all far from the bursty link's 0%. This makes the link appear bursty instead of independent in terms of distance.

As bursty and independent delivery are the two ends of the spectrum, we quantify burstiness in terms of the distance of the empirical link compared to the distance of an independent link with the same PRR. For brevity, we call this burstiness metric β:

$$\beta = \frac{KW(I) - KW(E)}{KW(I)}$$

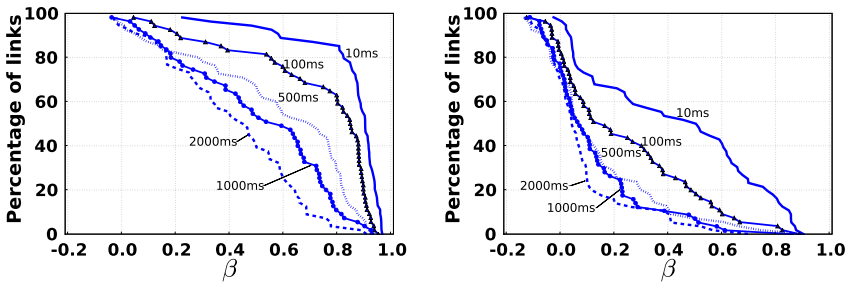

(a) Channel 26

(b) Channel 16

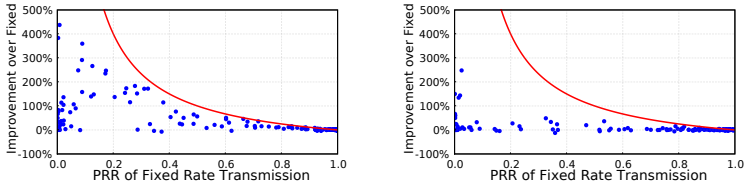

(c) Channel 26

(d) Channel 16

Figure 7. β and opportune transmissions performance in Mirage on channels 26 and 16. CCDF of β shown in (a)-(b) (up and to the right means more bursty). At an inter-packet interval of 10ms, more than 85% of the intermediate links have β above 0.80. On channel 16, which overlaps with a nearby 802.11 network, fewer than 15% of the links have β above 0.8 for any inter-packet interval. Channel 26 has more bursty links than channel 16. Improvements from opportune transmissions shown in (c)-(d) (the red curve shows the maximum possible improvement). Opportune transmissions work significantly better on channel 26 than on channel 16: channel 26 has over 25% of intermediate links improve by at least 100% while channel 16 has none.

where $KW()$ is the distance from the ideal bursty link, E is the CPDF of the empirical link in question, and I is the CPDF of an independent link with the same PRR.

Figure 6 shows a sample β calculation. The elements e_1 to e_6 are averaged to get KW(E) – the distance between an empirical link and the ideal bursty link. Similarly, i_1 through i_6 are averaged to obtain KW(I) – the distance between the corresponding independent link and the ideal bursty link. With these two values we can compute β using the formula above.

A perfectly bursty link has a β=1, while a link with independent deliveries has a β=0. To get a sense of what β looks like, the captions in Figure 4 include the corresponding β values of the four example links.

Note that negative β values are permitted. This happens when there is a negative correlation in packet reception: as more packets are received the next packet is more likely to fail and as more packets are lost the next packet is more likely to be received. Figure 5(b) shows the CPDF of one such link we measured.

3.4 Distributions of β

With a way to measure link burstiness, we can examine the distribution of β values of intermediate links to better understand how bursty a given network is. Figure 7(a) shows the complementary CDF (CCDF) of β values for intermediate Mirage links on channel 26. This plot is from the same data as Figure 4. By subsampling each 100,000 packet trace, we can calculate β for different inter-packet intervals (IPI).

Figure 7(a) shows that as the inter-packet interval increases, β decreases. At an IPI of 10ms, 40% of intermediate links have a β above 0.9. At 500ms and 1 second, however, fewer than 5% of the links have a β this high. Furthermore, the percentage of links that have a β close to zero increases as the inter-packet interval increases: no links at 10ms, 20% at 500ms and 25% at 1 second.

Section 2 noted that PRR distributions in the Mirage testbed differ based on channel. Figure 7(b) shows the CCDF of β values for channel 16 links. The percentage of links with $\beta > 0.9$ is less than one third that of channel 26 links (Figure 7(a). Still, channel 26 is the most commonly used channel for 802.15.4 protocol studies. The difference in the distribution of β on channel 16 suggests that the conclusions from such studies may not be generalizable to other channels.

3.5 Observations

The inverse relationship between the inter-packet interval and β means that sending packets further apart decreases the correlation between their fates. This correlation is in terms of both successful and failed transmissions. In networks which exhibit high β values, a failed packet transmission means that the chance of an immediate retransmission success is low. However, if a node waits long enough then probability of delivery will be independent of the prior loss.

A protocol that understands β can play the odds of

delivery, trading off latency to improve communication efficiency. Figure 7(a) shows that the percentage of intermediate links with β less than 0.20 is almost the same for inter packet intervals above 500ms: 17% for 500ms, 21% for 1 sec and 23% for 2 seconds. This suggests that waiting for 500ms represents the knee of the efficiency benefit curve in the Mirage network. The following section investigates if indeed β captures burstiness and explores if knowledge from β – the pause duration after a failure – can improve protocol performance.

4 Opportune Transmissions

This section presents a simple algorithm that increases the observed reception ratio of bursty links. A node sends packets as quickly as possible until a loss occurs. When a packet delivery fails, the node waits and this back-off gives the next packet an independent chance of delivery. While pausing breaks the packet loss correlation, sending packets back-to-back preserves the correlation between packet successes. We call this approach *opportune transmissions* because a node takes advantage of opportune moments of high reception.

4.1 Reception Ratio Improvement

First, we examine how opportune transmissions change single-hop link reception ratios. For each link in the 100,000 packet Mirage traces, we measure the PRR for fixed periodic transmission and for opportune transmissions. In the second case, upon a packet delivery success, a node sends back-to-back packets until a failure occurs. On a failure, the protocol waits until the next time the fixed period algorithm would transmit. We use this variable waiting period to a fixed point rather than waiting for a fixed period, because the latter introduces noise due to phase shifts. Both protocols send the same total number of packets.

Comparing fixed and opportune reception ratios shows whether a node can improve its efficiency by taking advantage of correlated successes. Figures 7(c) and 7(d) show how opportune transmissions affect the observed reception ratio on channels 26 and 16 of Mirage. We set the backoff inverval after failure to 500ms. On channel 26, many links see improvements, some to near-optimal levels, and a small number see minor degradations. For example, two links with fixed reception ratios of about 0.67 and 0.73 reach a reception ratio very close to 1. Comparing the performances on the two channels, opportune transmissions improves observed reception ratios by more than 100% on nearly 25% of the intermediate links on channel 26 and improves no links on channel 16.

Figure 8 plots improvement from opportune transmissions against β, with PRR shown in grayscale. Links with low PRR and high β see large improvements while low-β links do not see much improvement. The high PRR links with high β do not improve as much as the low PRR links because low PRR links have more room for improvement in terms of packet successes. Section 3 showed channel 26 has more high beta links than channel 16. β is capturing the differences in burstiness and can help understand why protocols similar to opportune transmissions, for exmaple OAR [25], behave differently on different networks.

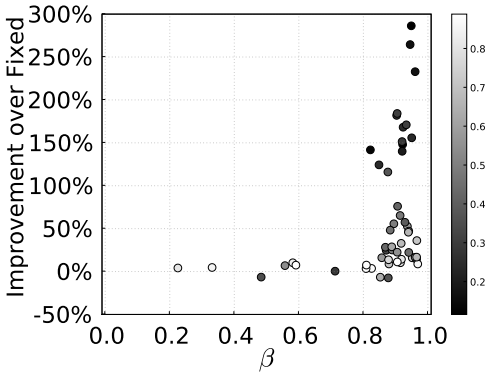

Figure 8. β and improvement in PRR due to opportune transmissions for all intermediate links on channel 26 of Mirage. Grayscale shows the the PRR from fixed transmissions. Links with low PRR and high β improve significantly. High PRR links don't have much to improve.

Figure 9 shows channel 26 improvements from opportune transmissions for different back-off intervals after a failure. Increasing the back-off garners larger reception ratio improvements because it decreases the correlation of packet delivery failures. As the results in Section 3 indicated, the knee of the curve in breaking correlations occurs at 500ms, after which the improvements level off. This leveling off is hard to see in Figure 9 due to the density of points with high fixed reception ratios, but later results show it more clearly.

4.2 End-to-End Path Improvement

Link improvements do not guarantee improvements in end-to-end routes. It may be that the improved links are irrelevant for low-cost routes. In other words, while β can tell us about protocol performance on single hop links, it may be irrelevant when end-to-end performance is considered. Therefore, we examine whether the link improvements observed in Figure 9 translate to lower end-to-end path costs.

Figure 10 compares the minimum-cost paths between all node pairs for fixed and opportune transmissions, where a link cost is its expected transmissions per delivery (ETX), or $\frac{1}{PRR}$. For a probe interval of 500ms, the mean improvement over all paths is about 4.5% with the maximum reaching 45%. Overall, using opportunistic transmissions decreases the least-cost path for nearly all node pairs, thus improving the network's transmission efficiency. While a 500ms pause causes significant improvements over the 100ms backoff interval (note the larger number of links with a fixed ETX of 2 and their downward shift), increasing the value to 1 second does not see significant further improvements.

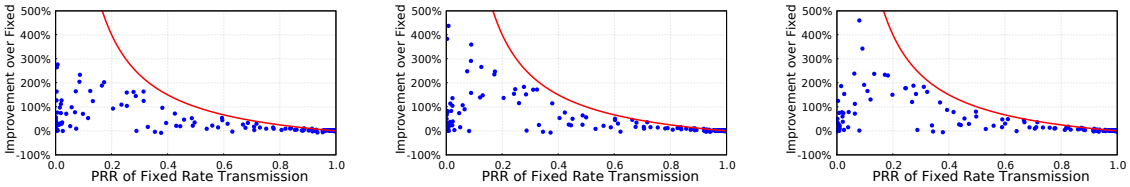

(a) IPI=100ms (b) IPI=500ms (c) IPI=1000ms

Figure 9. Improvements of opportunistic transmissions for different probe intervals on Channel 26 in Mirage. Increasing the probe interval to 500ms improves greatly over 100ms, but 1 second does not improve much further.

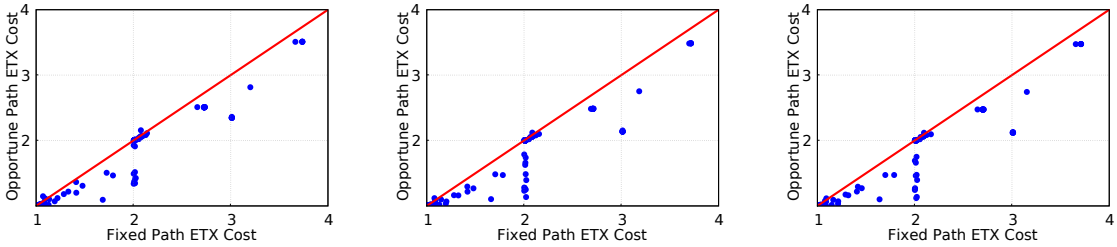

(a) IPI=100ms (b) IPI=500ms (c) IPI=1000ms

Figure 10. Opportune transmissions improve the path ETX in Mirage (lower is better).

4.3 Lower Transmit Power

The end-to-end results so far are from datatraces obtained on a strongly connected network, where each Mirage node transmits at 0dBm and the maximum ETX path of 4. As a simple sanity check of whether our observations have overfit to a particular network trace, we examine what happens in a more loosely connected network.

Figure 12 shows end-to-end ETX measurements when nodes transmit at -15dBm for fixed and opportune transmissions. For most paths, the reduction in ETX is small. For several paths, however, the reduction is dramatic – up to 90%! A linear shift of the data points in the lower right of the figure suggests that a number of paths have improved due to one link's improvement. This suggests that mesh protocols that seek to minimize route cost can see significant benefits from even a small number of link improvements.

4.4 Three Caveats

The end-to-end study carried out in this section provides evidence that β is useful in understanding and improving protocol performance. Opportune transmissions see significant improvement in reception ratios when pausing for 500ms after a packet loss, the same value that we inferred from the decay of β in Section 3. While these results are promising, three aspects of our methodology prevent us from generalizing applicability of β to real-world wireless protocols:

• Figure 2 showed that two other 802.15.4 testbeds see PRR distribution shifts similar to Mirage's but generalizing our results to 802.15.4 networks as a whole requires understanding the causes of burstiness and its network prevalence.

• Even if burstiness is a general phenomenon in 802.15.4, there are many other link layers. It could be that β is only relevant in 802.15.4. Understanding which link layers have high β values and which do not can provide a quantitative basis for making different protocol decisions. Furthermore, if the applicability is not uniform, this introduces challenges in cleanly abstracting wireless to higher-layer protocols.

• Data traces are not representative of real network traffic. In the traces of 100,000 broadcasts, for example, each set of broadcasts (and therefore link measurements) occurred 15 minutes apart, yet when we compute minimum-cost paths we assume they were taken at the same time. Furthermore, the analysis so far assumes a protocol has perfect knowledge of whether a packet was delivered; in real networks a protocol must rely on possibly lossy link-layer acknowledgements. Concluding whether β can be used to tune protocol parameters requires measuring a protocol on a real network.

The next three sections address these caveats in turn, examining the causes of link burstiness and β's applicability to link layers other than 15.4.

5 Causes of Burstiness

We find that bursty links are often links on the edge of reception sensitivity, such that small 1-2dB swings in signal strength significantly change the observed packet reception ratio.

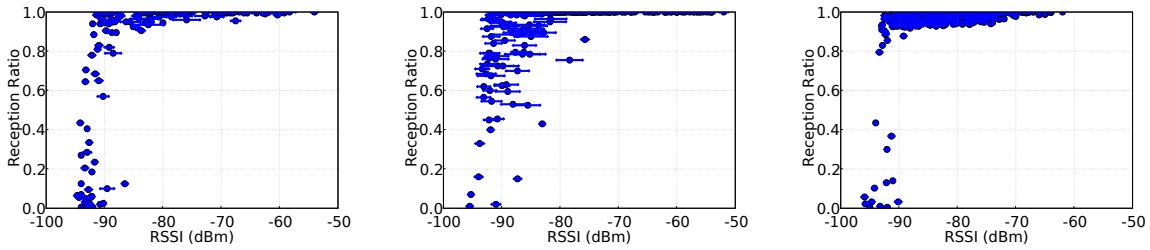

(a) Mirage. (b) Lake. (c) University.

Figure 11. Packet reception ratio versus received signal strength on channel 26 with IPI=50ms. Each data point is for a directional node pair. The average RSSI is marked by circles and the error bars show one standard deviation. Overall, RSSI and reception ratio correlation is similar across different testbeds with some outliers.

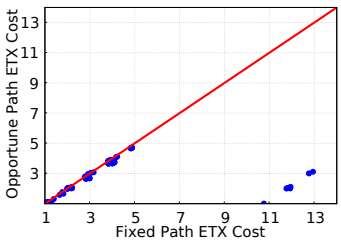

Figure 12. ETX improvements at -15dBm and a packet interval of 500ms. A number of paths all experience a constant shift ETX reduction of approximately 90%. This suggests that they all shared a single link which opportune transmissions improved greatly.

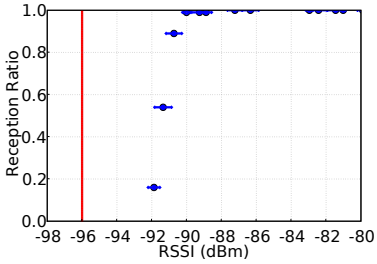

Figure 13. PRR versus RSSI plots for two nodes connected through a variable attenuator. The red line shows the noise floor of the receiving node. Intermediate PRRs are within 1.5dB range.

5.1 Received Signal Strength Indicator (RSSI)

Figure 11 plots the signal strength of received packets against link reception ratio. In all three testbeds there is a general trend: if the mean received signal strength (RSSI) [6] is above -80dBm then the link is almost always good. The two exceptions occur in the lake testbed, where people were actively moving between the nodes. Below -80dBm, there is a grey region of good, intermediate, and poor links [27].

To understand this grey region better, we followed Aguayo et al.'s methodology [2], wiring two nodes together through a variable attenuator via shielded SMA cables. At each attenuation level (1dB to 64dB) one node transmitted 100 packets with an inter-packet interval of 50ms. The receiver logged the RSSI and sequence number of received packets to its flash. We measured background (hardware/AWGN) noise by sampling the RSSI register of the CC2420 of both nodes when there was no traffic. Then we calculated the noise floor as the mode of these samples.

Figure 13 shows that there is a crisp RSSI/PRR curve. The small error bars show that the RSSI at each attenuation level is stable. The receiver does not receive any packets below a signal to noise ratio of 4dB. All of the intermediate PRRs are within a 1.5 dBm range from -92 to -90.5dBm. If the signal strength is close to the noise floor, a 1.5dB shift can change it from a good link to a bad link and vice versa. We repeated this experiment for two separate node pairs, and both had near-identical 4dB signal-to-noise thresholds and intermediate link windows of 1.5 dB.

However, not all nodes have the same noise floor. In the attenuator experiment, one node had a noise floor of -98dBm and observed a good link at -92dBm; the node in Figure 13 had a noise floor of -96dBm and observed a good link at -90dBm. Across a large network, this variation can be large. In the Mirage testbed experiment in Figure 11(a), 5 nodes had noise floors at -98dBm, 8 at -97dBm, 4 at -96dBm, 3 at -95dBm, 2 at -94dBm, 3 at -93dBm and 1 at -92dBm. Therefore, even if every node observes a crisp signal-to-noise/packet reception curve, the threshold values for these curves are spread across 6dB. While the broad spread is partially due to the fact that these are very inexpensive, low-power radios, examining datasets from the Roofnet 802.11b mesh [2], we saw a 6dB spread in noise floors, albeit with 80% of the nodes having the same value.

Noise floor variations only partially explain the grey region. Its range (-85dBm to -96dBm: 11dB) is greater than the range of the noise floors (-98dBm to -92dBm: 6dB). We believe this additional 5dB of range is due

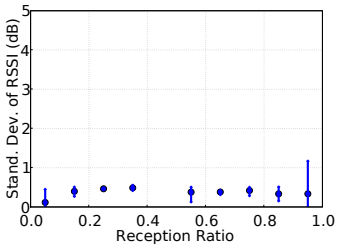

(a) Mirage, IPI = 10ms, Channel 26.

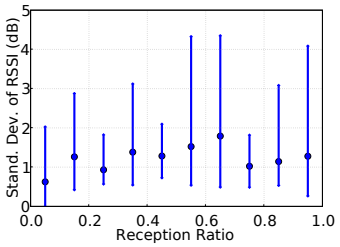

(b) Mirage, IPI = 14s, Channel 26.

Figure 14. The plot shows mean, max and min RSSI observed at different reception ratios. Each data point is a bin of all links within a 10% range: the fourth data point, for example, is 30-40%. RSSI is stable for short term traffic and varies more over longer time periods.

to an inherent measurement bias common to all such studies: nodes only measure the signal strength of received packets. If there are 6-7dB changes in signal strength, then link may transition from good to non-existent, yet the receiver will see only the RSSI of a good link. The comparatively short range and low bit rate of 802.15.4 means it does not observe the same multipath inter-symbol self-interference observed in Roofnet's 802.11b [2]. Nevertheless, we cannot definitively explain the entire width of the grey region, and leave such investigations to future work with software radios.

Figure 14 plots the minimum, mean and the maximum standard deviations of RSSI of different reception ratios for inter-packet intervals of 10ms and 14s in the Mirage testbed. With 10ms intervals, the average standard deviation is below 1dB across all PRRs for all links and the maximum is 1.5dB. With 14 second intervals, the average standard deviation is more than 1dB for all links with a reception ratio above 0.1 and the maximum is as high as 4.2dB.

The stability of RSSI over short time spans and its variation over longer time spans suggests that the channel variations may be the cause of burstiness. Figure 15 shows a detailed look at the RSSI for a sequence of received packets for an intermediate link. While most of the received packets have an RSSI of at least -94dBm, a few are as low as -95dBm. If a link is near the cusp of reception sensitivity, then slight variations can cause

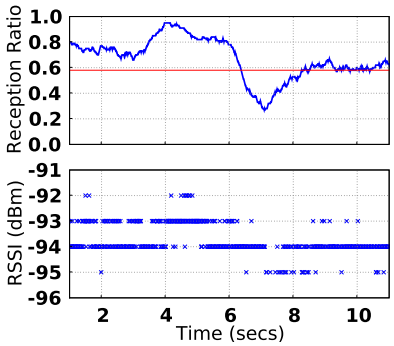

Figure 15. RSSI and PRR variations over time on a single link. The PRR over time is from a sliding window of size 100. Red horizontal line in the PRR plot shows the overall average PRR of the link. The RSSI oscillates with scattered reception close to -95dBm and denser reception above. The clustered reception and losses show the burstiness of the link.

packet losses and make the link intermediate. Figure 15 shows a dip in the reception ratio just after 7 seconds. This dip happens after weak packets with RSSI close to -95dBm. There are no reception ratio dips when strong packets are received. This shows that the losses were not due to external interference. Clustered receptions such as these are common in high β links, and are a dominant cause of link burstiness. RSSI shifts of this kind are typical of all but the most controlled environments, either due to environmental effects [21] or simple multipath fading.

5.2 Burstiness and Interference

Figure 3 and Figure 7(a) showed that Mirage has more intermediate links on channel 16 than 26. The university testbed observed a similar shift, while we found channel choice did not affect the link distribution in the lake testbed. In Mirage, this change in link distribution is accompanied by much lower β values on channel 16. This change in β is due to interfering 802.11 transmissions. Channel 16 is in the middle of 802.11b channel 6, while channel 26 is outside the spectrum used by 802.11b [26].

Figure 16 shows 1kHz noise samples at a single node on channels 16 and 26 in Mirage. There were no 802.15.4 transmissions during these measurements. While channel 16 shows large spikes, channel 26 shows none. Because these spikes of 802.11 traffic are independent of 802.15.4 transmissions, they appear to 802.15.4 nodes as independent packet losses. The university testbed also has nearby 802.11b, and therefore observes similar external interference. The lake testbed, in contrast, has very little 802.11 interference and so burstiness is unaffected by the choice of channels.

6 Other Link Layers

Section 5 showed that channel variation is a possible cause of burstiness, suggesting β may be applicable to

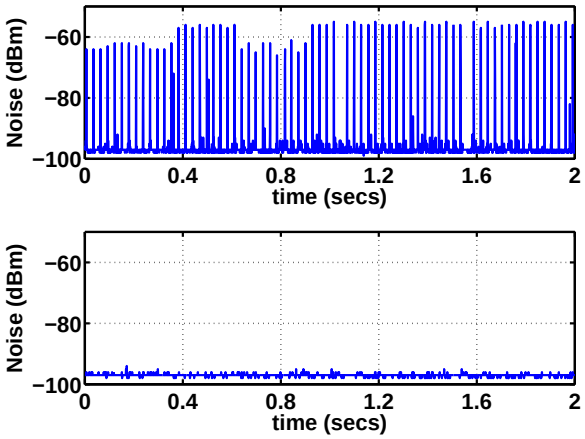

Figure 16. High frequency noise samples on channels 16 (top) and 26 (bottom) in Mirage. No 802.15.4 nodes were transmitting. Channel 16 shows large spikes while channel 26 is quiet.

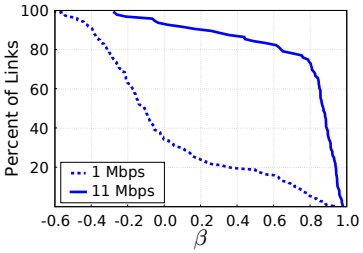

Figure 17. Complementary CDFs of β for links in the 11Mbps and 1Mbps Roofnet data (up and to the right is more bursty). 11Mbps links are highly bursty, while 1Mbps links show very low β values. This suggests that 1Mbps data will not benefit from opportune transmissions and that 11Mbps data will.

link layers other than 802.15.4. This section analyzes 802.11b packet traces from two recent SIGCOMM publications, one from the Roofnet project at MIT [2] and the other from the University of Washington [23]. The Roofnet dataset is a large-scale outdoor 802.11b mesh, while the Washington dataset is a small indoor testbed. We measure β using these traces and compute the link as well as the end-to-end efficiency improvements.

6.1 Roofnet: Outdoor 802.11b

Figure 17 shows the complementary CDF of β values from the 1Mbps and 11Mbps Roofnet SIGCOMM packet traces. At 11Mbps, about 20% of the links have a β of 0.8 or higher. At 1Mbps, on the other hand, less than 2% of the links have β above 0.8. Furthermore, 40% of the 1Mbps links observe a negative β value, indicating a negative correlation between past and future packet events. While high β values are not unique to 802.15.4, not all link layers exhibit them.

Figures 18(a) and 18(b) show how opportune transmissions affect link quality in Roofnet. The 11Mbps

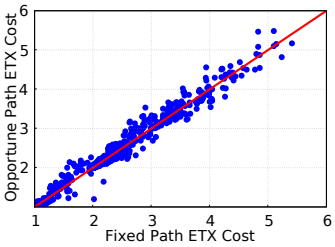

Figure 19. Opportune transmissions do not decrease end-to-end ETX in Roofnet at 1Mbps.

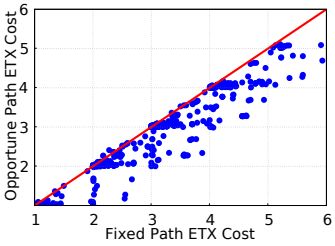

Figure 20. Opportune transmissions decrease end-to-end ETX in Roofnet at 11Mbps. Some routes see 50% reductions in cost.

data, having many links with high β values, benefits from opportune transmissions. The 1Mbps data set, in contrast, sees many links whose quality degrades with opportune transmissions. This is due to negative β values: pausing after a failure reduces the chances that the next packet will succeed.

Figures 19 and 20 show results for end-to-end ETX paths. 1Mbps is consistent with the link improvement results and shows that few paths improve while most degrade due to the decrease of link packet reception ratio. On the other hand, the 11Mbps paths show an average improvement of about 6% with a maximum improvement of 54%: these results are very similar to those in Mirage.

6.2 Washington: Indoor 802.11b

The Washington testbed is interesting because it is located inside a building with many sources of interference (e.g people, microwave ovens, and building-wide 802.11). Figure 18(c) shows the link quality improvement for the 8 1Mbps links. One of the intermediate links experiences a 200% increase in reception ratio (0.2 to 0.6). The small number of links and single-hop nature of the experiment precludes computing end-to-end costs or β distributions. However, this data suggests that if more nodes are deployed and each node were a sender, we would see end-to-end path ETX reduction in the opportune transmissions approach. At 1Mbps, Roofnet sees no benefit from transmitting opportunely, but the 1Mbps Washington testbed has noticeable improvements.

Overall, we can conclude that β can capture bursti-

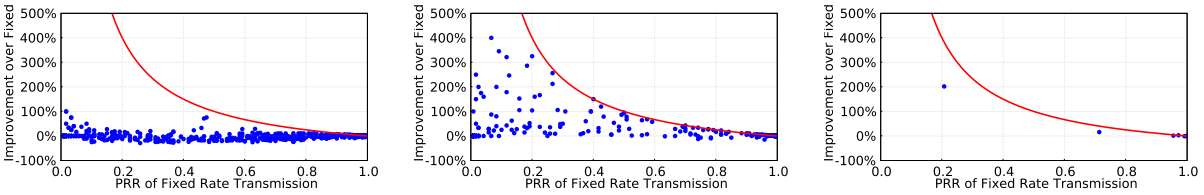

(a) 1Mbps Roofnet (b) 11Mbps Roofnet (c) 1Mbps Washington

Figure 18. While 1Mbps Roofnet sees many links degrade with opportune transmissions, 11Mbps Roofnet and Washington both observe significant link improvements. The Roofnet results are consistent with the low β values in Figure 17.

ness and can predict protocol preformance in link layers other than 802.15.4. This shows the broader applicability of β.

7 Protocol Improvements

Sections 4 and 6 have shown that networks with high-β links see reduction in path costs if a protocol pauses after a failed transmission. So far, results have been based on packet traces which we used to measure β. This section examines whether knowledge from β can predict how an approach similar to opportune transmissions performs in a real testbed experiment after measuring β. We show that changing the back-off constant in TinyOS 2.0's Collection Tree Protocol (CTP) [9] implementation reduces its end-to-end delivery costs by 15% on Mirage's channel 26, a network with high-β links.

7.1 CTP

The Collection Tree Protocol (CTP) is the standard TinyOS 2.0 data collection protocol that provides a reliable anycast service to data sinks using an agile link estimator. At the single-hop level, CTP uses two timer values to regulate data rates. The first, the success interval, is how long CTP waits after it sends a packet and receives the link-layer acknowledgement. The second, the no-ack interval, is how long CTP waits after it sends an unacknowledged packet. For the 802.15.4 MAC in TinyOS, both intervals are 16-31ms, which is approximately 1-2 packet times.

To examine whether measuring β can improve CTP's efficiency, we modified the no-ack interval to be a fixed 500ms. This value is chosen based on β observations made earlier.

7.2 Results

To measure the effect of this change, we ran CTP on 80 nodes on the Intel Mirage testbed at two transmission power levels on channel 26. Each node generated a data packet every 10 seconds. CTP had a single collection root, located at one corner of the network. Each node sent 128 packets, for a total runtime of 21 minutes. Because CTP discovers topology quickly, we measured receptions once every node had delivered a packet to the root: in every case the counts begin at the fifth packet.

	-7dBm	-15dBm
Immediate	4.73	6.71
Opportune	4.02	5.65
Reduction	15%	15%

Figure 21. Effects that β has on the average routing cost (transmissions/delivery) for CTP at two transmit power levels. A back-off of 500ms reduces the average cost by 15%.

We measured routing cost by logging every packet reception and transmission to Mirage's wired backchannel. By counting the number of transmissions and dividing by the number of unique packets the root receives, we can measure the average number of transmissions per delivery.

Figure 21 shows the results – by waiting 500ms after an unacknowledged packet, CTP's average delivery cost drops by 15%. This is larger than the results in Section 4, which calculated average improvements over an entire network to be 2%-4%. This difference stems from the time scale of the experiments. The trace-based results in Section 4 measured the minimum cost path based on the PRR of an entire trace, while CTP may change its next hop as often as every five data packets. As high β values cause links to come and go, CTP can dynamically take advantage of active good links.

To measure the distribution of path effects, we measured the difference in single-hop and route ETX for each node. A node's single-hop ETX is the number of packets it transmitted divided by the number that were acknowledged [2]. A node's path ETX is the transmission count across the entire network for packets it originated, divided by the number of unique packets received at the collection root.

Figure 22 shows the results. Overall, the link improvements are negligible. While 20% of the −15dBm nodes observe improvements of 10% or more, just as many -7dBm nodes observe a 10% degradation. The average improvement at -15dBm is 1.2%, while at -7dBm the average is a 0.5% degradation.

Despite these anemic link-layer results, both power

[2] As false positive acknowledgements are $< 0.1\%$ of packets and uniformly distributed, we ignore them for simplicity.

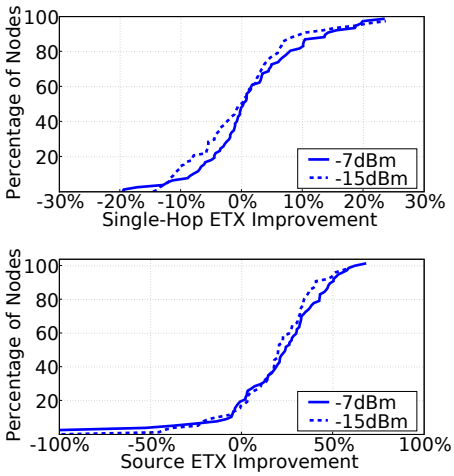

Figure 22. CDF of ETX improvements at the first hop and end-to-end. The average link improvement is ±1%, but the average end-to-end improvement is ≈15%. The large end-to-end degradations reflect a few nodes having different length routes in the two experiments.

levels see significant end-to-end improvements. A small number of nodes see large (≈100%) degradations because they have 2-hop, rather than 1-hop, routes. Because the two experiments ran at different times, it is hard to determine if these changes were due to the backoff or the underlying channel. Nevertheless, these outliers are more than made up for by nodes whose routes shorten or become more efficient: the 80^{th} percentile sees route cost reductions of 34-42%. This causes an overall improvement of 15% while the reliability in all cases was 96-97%.

For the high-power CTP experiment, the maximum observed end-to-end packet latency when transmitting opportunely was 4 seconds; in the low-power experiment it was 25 seconds. All packets arrived in under 1 second with immediate transmissions. Clearly, sending packets in burst and pausing after a failure affects reception latency, but this is an acceptable tradeoff for certain sensornet applications.

CTP's route selection explains the seemingly contrary link layer and end-to-end results. While the average link-layer improvement is close to zero, nodes do not have a uniform transmission load. In seeking the minimum-cost path, CTP automatically selects nodes with improved links. Even though backing-off only improves 40% of the links in the network, higher layer protocols then preferentially use these links, leading to significant overall improvements. This result echoes what was observed in Figure 12, where a single link improvement reduced a number of routes by 80% or more.

The 15% reduction in transmission cost just by changing a single parameter in CTP affirms that knowledge of β can be used to improve protocol performance.

8 Related Work and Discussion

This paper shows that many but not all link layers observe burstiness. It presents β – an effective way to measure this burstiness. Looking at the improvements of network performance using opportune transmissions we show that measuring β can help understand why protocols behave differently on different networks. It further explores the causes of burstiness and shows that it is due to channel variations; this makes β relevant to 802.11 wireless networks, in addition to the 802.15.4 ones. Finally, tuning the failure backoff timer of CTP is an example of how β can help protocol designers tune parameters to improve network performance.

Our observation that wireless links have a strong temporal component is not new: Roofnet and other sensornet studies have observed similar behavior. The challenges caused by the combination of correlated losses (described in Section 2), as well as independent losses like those observed on the SNR/PRR knee in Figure 11, led Noble et al. to propose a suite of link estimators, some of which flip-flop between different estimation time scales [18]. Other sensornet link estimators take similar approaches [29]. While the observation that links have temporal correlation is not new, methodology to measure burstiness is.

Autocorrelation and burst length distributions could be alternatives to CPDFs, but they are not as powerful. Autocorrelation does not distinguish burst of successes from burst of failures. CPDFs look at these seperately, and are therefore more informative than autocorrelation. Using burst length distributions to quantify burstiness, on the other hand, is hard, as they are prominent only at small burst lengths. While small variations in the burst length distribution at large lengths are important when we study burstiness, they are hard to detect. For example, a link with independent reception except for a single large burst of losses will show no significant deviation in the burst length distribution from that of an independent link without any burst of losses. A CPDF will make the distinction between the two links more observable.

A burstiness parameter, widely used in wireless analysis, is μ, which is from the Gillbert-Elliot channel. μ is calculated from the transitional probabilities of the G-E model in which the good state corresponds to 100% packet reception and the bad state corresponds to 0% packet reception. The equation to calculate μ is given by

$$\mu = 1 - P_{gb} - P_{bg} \quad (1)$$

where, P_{gb} and P_{bg} are the probabilities of transitioning from good to bad state and from bad to good state respectively. Thus, μ captures the correlation between the current and the previous packet delivery events. It does not capture how correlated the current packet delivery event is to several packets in the past. CPDF, on the other hand, does capture such correlations by looking at the probability of the current packet succeeding given several previous packets succeeding or failing. In

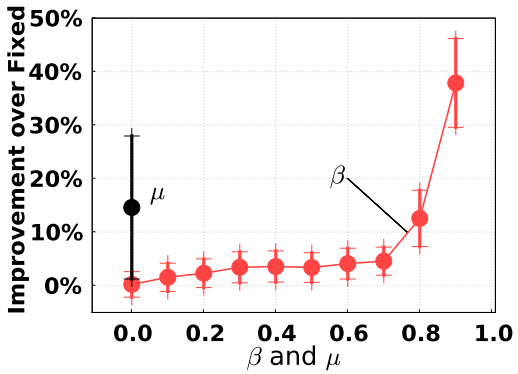

Figure 23. Comparing improvements from opportune transmissions with β and μ for synthetic links with PRR = 0.5. Links have independent reception except for a randomly placed burst of successes. The y-axis shows the improvements from opportune transmissions compared to fixed transmissions. The circles show the average and bars show one standard deviation of all links with β (μ) within 0.05 from a given β (μ) on the x-axis. Average improvements (circles) increase with an increase in β. μ for all the links is around 0.

fact, μ can be calculated from two elements of a CPDF: μ = CPDF(1) - CPDF(-1). Thus, β, which is calculated from the CPDF, may be thought of as a generalization of μ.

Figure 23 shows the observed reception ratio improvements from opportune transmissions vs. β and μ. As this improvement depends on the overall PRR of a link, we look at links with a fixed PRR (of 0.5) to do a fair comparison between β and μ. We use synthetically generated data traces in which links have independent reception except for a single burst of successes; the size of the burst vary from trace to trace. The location of the burst affects the improvement opportune transmissions observe. For example, if opportune transmission catches the begining of this burst then it will make use of the entire burst, which will significantly favor opportune transmissions over the fixed transmissions. Therefore, we randomized the burst location in every trace and generated 100 such traces for every burst size.

Figure 23 shows that an increase in β corresponds to an increase in the improvement from opportune transmissions. However, μ is always close to 0 regardless of the burstsize. This shows that β is a better measure of burstiness than μ.

More recently, Aguayo et al. [2] used Allan deviation of reception rates calculated over different time intervals to find the characteristic burst length of a link: the Allan deviation will be high for interval lengths near the characteristic burst length and will be small at smaller and longer intervals. We did not observe this pattern in the Allan deviation plots for the links from the Mirage testbed.

There is also work in modeling packet burstiness in wired LANs, for example, with packet trains [15]. Such models may be extended and used for packet burstiness in wireless links. There is also a long history of modeling wireless links as *n*-state or *n*-stage Markov models [3, 11]. The variety and complexity of CPDFs we observe show that these models can capture some, but not all of the important behaviors in wireless networks. Furthermore, we do not go so far as to model communication based on CPDFs. In this paper, we only try to measure burstiness and not model it. At the very least, we have yet to look into how reception shifts across different node pairs are correlated (something the Markov models typically ignore), an area of future work we are interested in.

Some MAC layers resemble opportune transmissions in their behavior [1, 28, 25]. For example, 802.11b's exponential backoff in response to dropped acknowledgements can been seen as a logarithmic search for a good pause interval. However, these backoffs are not on the order of 500ms observed by β.

These results suggest that we should rethink how we model and design protocols for wireless networks. Protocols do not only need to decide where to send a packet, they also need to decide when to send a packet: the packet loss rate between two nodes is not independent of packet timing. Barring opportune reception schemes, lost packets are wastes of the wireless channel. If the link layer wishes to reduce transmission cost, it should use an algorithm similar to opportune transmissions – for example, OAR [25] – when scheduling packets. Rather than retry a failed packet immediately, a node can send packets with other destinations for a suitable pause interval. While these timing decisions are probably best handled at the MAC layer, network layers may wish to choose different destinations if there may be a large latency. "Cross-layer design" is often praised as an important technique for improving wireless networks [8, 16, 10]: β provides strong evidence that simple information flow on packet timing has significant benefits.

Acknowledgements

We would like to thank the anonymous reviewers for their useful reviews and Prof. Deepak Ganesan for shepherding this paper. We would also like to thank Mayank Jain, Prabal Dutta and Arsalan Tavakoli for insightful discussions.

This work was supported by generous gifts from Microsoft Research, Intel Research, DoCoMo Capital, Foundation Capital, the National Science Foundation under grants #0615308 ("CSR-EHS") and #0627126 ("NeTS-NOSS"), and a Stanford Terman Fellowship.

9 References

[1] ANSI/IEEE Std 802.11 1999 Edition.

[2] D. Aguayo, J. C. Bicket, S. Biswas, G. Judd, and R. Morris. Link-level measurements from an 802.11b mesh network. In *SIGCOMM*, pages 121–132, 2004.

[3] A. Cerpa. Low-power wireless links properties: Modeling and applications in sensor networks. In *PhD thesis, University of California, Los Angeles, California*, 2005.

[4] A. Cerpa, N. Busek, and D. Estrin. Scale: A tool for simple connectivity assessment in lossy environments. Technical Report 0021, Sept. 2003.

[5] A. Cerpa, J. L. Wong, M. Potkonjak, and D. Estrin. Temporal properties of low power wireless links: modeling and implications on multi-hop routing. In *MobiHoc '05: Proceedings of the 6th ACM international symposium on Mobile ad hoc networking and computing*, 2005.

[6] ChipCon Inc. CC2420 Data Sheet. `http://www.chipcon.com/files/CC2420_Data_Sheet_1_4.pdf`, 2006.

[7] D. S. J. D. Couto, D. Aguayo, J. Bicket, and R. Morris. A high-throughput path metric for multi-hop wireless routing. In *MobiCom '03: Proceedings of the 9th annual international conference on Mobile computing and networking*, 2003.

[8] S. Cui and A. J. Goldsmith. Cross-layer design of energy-constrained networks using cooperative mimo techniques. *Signal Process.*, 86(8):1804–1814, 2006.

[9] R. Fonseca, O. Gnawali, K. Jamieson, S. Kim, P. Levis, and A. Woo. TEP 123: Collection Tree Protocol. http://www.tinyos.net/tinyos-2.x/doc/.

[10] R. Fonseca, O. Gnawali, K. Jamieson, and P. Levis. "four bit wireless link estimation. In *The Sixth Workshop on Hot Topics in Networks (HotNets-VI)*, Nov. 2007.

[11] E. N. Gilbert. Capacity of a burst-noise channel. *Bell System Tecnical Journal*, 39:1253–1266, 1960.

[12] A. Goldsmith. *Wireless Communications*. Cambridge University Press, New York, NY, USA, 2005.

[13] J. Hill, R. Szewczyk, A. Woo, S. Hollar, D. E. Culler, and K. S. J. Pister. System Architecture Directions for Networked Sensors. In *Architectural Support for Programming Languages and Operating Systems*, pages 93–104, 2000. TinyOS is available at http://webs.cs.berkeley.edu.

[14] Intel Research Berkeley. Mirage testbed. `https://mirage.berkeley.intel-research.net/`.

[15] R. Jain and S. Routhier. Packet trains–measurements and a new model for computer network traffic. In *IEEE Journal on Selected Areas in coomunications*, volume 4, September 1986.

[16] K. Jamieson and H. Balakrishnan. PPR: Partial Packet Recovery for Wireless Networks. In *ACM SIGCOMM*, Kyoto, Japan, August 2007.

[17] C. Jiao, L. Schwiebert, and B. Xu. On modeling the packet error statistics in bursty channels. In *LCN '02: Proceedings of the 27th Annual IEEE Conference on Local Computer Networks*, pages 534–541, Washington, DC, USA, 2002. IEEE Computer Society.

[18] M. Kim and B. Noble. Mobile network estimation. In *MobiCom '01: Proceedings of the 7th annual international conference on Mobile computing and networking*, pages 298–309, New York, NY, USA, 2001. ACM Press.

[19] A. Köpke, A. Willig, and H. Karl. Chaotic maps as parsimonious bit error models of wireless channels. In *Proc. of IEEE INFOCOM*, San Francisco, USA, Mar. 2003.

[20] H. Lee, A. Cerpa, and P. Levis. Improving wireless simulation through noise modeling. In *IPSN '07: Proceedings of the 6th international conference on Information processing in sensor networks*, 2007.

[21] S. Lin, J. Zhang, G. Zhou, L. Gu, J. A. Stankovic, and T. He. Atpc: adaptive transmission power control for wireless sensor networks. In *Proceedings of the 4th international conference on Embedded networked sensor systems*, pages 223 – 236, 2006.

[22] M. Mushkin and I. Bar-David. Capacity and Coding for the Gilbert- Elliott Channels. *IEEE Transactions on Information Theory*, 35:1277–1290, 1989.

[23] C. Reis, R. Mahajan, M. Rodrig, D. Wetherall, and J. Zahorjan. Measurement-based models of delivery and interference in static wireless networks. In *SIGCOMM*, pages 51–62, 2006.

[24] Y. Rubner, C. Tomasi, and L. J. Guibas. A metric for distributions with applications to image databases. In *Proceedings of the IEEE International Conference on Computer Vision*, pages 59–66, 1998.

[25] B. Sadeghi, V. Kanodia, A. Sabharwal, and E. Knightly. Oar: an opportunistic auto-rate media access protocol for ad hoc networks. *Wirel. Netw.*, 11(1-2):39–53, 2005.

[26] K. Srinivasan, P. Dutta, A. Tavakoli, and P. Levis. Some implications of low power wireless to ip networking. In *The Fifth Workshop on Hot Topics in Networks (HotNets-V)*, Nov. 2006.

[27] K. Srinivasan and P. Levis. Rssi is under appreciated. In *Proceedings of the Third ACM Workshop on Embedded Networked Sensors (EmNets 2006)*, May 2006.

[28] The Institute of Electrical and Electronics Engineers, Inc. Part 15.4: Wireless Medium Access Control (MAC) and Physical Layer (PHY) Specifications for Low-Rate Wireless Personal Area Networks (LR-WPANs), Oct. 2003.

[29] A. Woo and D. Culler. Evaluation of efficient link reliability estimators for low-power wireless networks. Technical report, UC-Berkeley, November 2003.